Molecular Phylogenetics and Evolution
Vol. 17, No. 2, November, pp. 219–230, 2000
doi:10.1006/mpev.2000.0838, available online at http://www.idealibrary.com on IDEAL®

Diversity and Phylogenetic Implications of CsCl Profiles from Rodent DNAs

Christophe Douady,*,†,[1] Nicolas Carels,*,‡ Oliver Clay,*,‡
François Catzeflis,† and Giorgio Bernardi*,‡,[2]

*Laboratoire de Génétique Moléculaire, Institut Jacques Monod, Tour 43, 2 Place Jussieu, F-75005 Paris, France; †Équipe Phylogénie Moléculaire, Laboratoire de Paléontologie, Institut des Sciences de l'Évolution, UMR 5554/UA 327, CNRS, Université de Montpellier II, Case 064, Place Eugène Bataillon, F-34095 Montpellier cedex, France; and ‡Stazione Zoologica Anton Dohrn, Villa Comunale, I-80121 Naples, Italy

Received December 13, 1999; revised July 17, 2000

Buoyant density profiles of high-molecular-weight DNAs sedimented in CsCl gradients, i.e., compositional distributions of 50- to 100-kb genomic fragments, have revealed a clear difference between the murids so far studied and most other mammals, including other rodents. Sequence analyses have revealed other, related, compositional differences between murids and nonmurids. In the present study, we obtained CsCl profiles of 17 rodent species representing 13 families. The modal buoyant densities obtained for rodents span the full range of values observed in other eutherians. More remarkably, the skewness (asymmetry, mean − modal buoyant density) of the rodent profiles extends to values well below those of other eutherians. Scatterplots of these and related CsCl profile parameters show groups of rodent families that agree largely with established rodent taxonomy, in particular with the monophyly of the Geomyoidea superfamily and the position of the Dipodidae family within the Myomorpha. In contrast, while confirming and extending previously reported differences between the profiles of Myomorpha and those of other rodents, the CsCl data question a traditional hypothesis positing Gliridae within Myomorpha, as does the recently sequenced mitochondrial genome of dormouse. Analysis of CsCl profiles is presented here as a rapid, robust method for exploring rodent and other vertebrate systematics. © 2000 Academic Press

Key Words: **DNA; phylogeny; ultracentrifugation; genomes; base composition; rodents; vertebrates; Eutheria; evolution.**

INTRODUCTION

The long, compositionally homogeneous regions of which mammalian genomes consist, the isochores (⩾300 kb on average), belong to a small number of families. Within any isochore family, GC levels[3] of 50- to 100-kb regions, or fragments, vary little (2–3% GC); yet, together these isochore families span a wide GC range, from 30 to 60% (Macaya *et al.*, 1976; Thiery *et al.*, 1976; Cuny *et al.*, 1981; Bernardi *et al.*, 1985; reviewed in Bernardi, 1995, 2000).

A buoyant density profile of genomic fragments, obtained by analytical ultracentrifugation of total nuclear DNA to sedimentation equilibrium in CsCl density gradients, yields the distribution of the GC levels of the fragments, since buoyant density and GC of DNA are linearly related (Schildkraut *et al.*, 1962). In the present work, with the knowledge of eukaryotic genomes acquired using sequence-specific ligands over three decades, we reexamine the potential of screening CsCl profiles of total nuclear DNA, without further fractionation or satellite analysis, as a tool for deducing and clarifying mammalian phylogenies. This approach was extensively used in previous work (see Bernardi, 1995, 2000 for reviews).

For comparisons between vertebrate species, the major Gaussian components provide a robust characterization of a species' genome. All studies so far indicate that there exists an invariant compositional pattern of a genome or species, independent of the presence or absence of satellite DNA and of molecular weight differences among DNA samples, that can be defined in terms of the Gaussian components of the CsCl profile's main band, excluding satellite DNA. It is the set of relative amplitudes (amounts of DNA) and GC contents (or buoyant densities, ρ) of these major compo-

[1] Present address: Medical Biology Centre, Biology & Biochemistry, Queen's University, 97 Lisburn Road, Belfast BT9 7BL, Northern Ireland.

[2] To whom correspondence should be addressed. E-mail: bernardi@alpha.szn.it.

[3] Abbreviations used: GC, molar fraction of guanine and cytosine in DNA; ρ, buoyant density; ρ_0, modal buoyant density; $\langle\rho\rangle$, mean buoyant density.

1055-7903/00 $35.00
Copyright © 2000 by Academic Press
All rights of reproduction in any form reserved.

nents. The compositional pattern of a species' genome is usually shown as a bar plot (see, e.g., Macaya *et al.*, 1976; Bernardi *et al.*, 1985; Cuny *et al.*, 1981; Bernardi, 1995) or, alternatively, as a set of partially overlapping Gaussian curves (Bernardi, 2000). Identifying the satellite DNA, finding the major components (i.e., calculating the compositional pattern), and inferring the relative numbers of genes in them are key steps in understanding a species at the genome level.

A compositional pattern's overall shape can often be estimated directly from a total DNA CsCl profile, without additional satellite information or fractionation. Moreover, as the present study confirms in the case of rodents, these CsCl profiles can furnish robust, rapidly obtainable, and potentially powerful information for systematics at the higher taxon levels (families, superfamilies, infraorders, and suborders). Similar analyses should also be possible for other orders. For example, bats (Chiroptera) exhibit an intraordinal variability of CsCl buoyant densities that appears to correlate with taxonomy, for Megachiroptera (flying foxes) have consistently lower modal buoyant densities (GC levels) than Microchiroptera (echolocating microbats) (Arrighi *et al.*, 1972; Pettigrew and Kirsch, 1995).

Previous studies of the compositional distributions of DNA fragments and genes from eutherian genomes have revealed the existence of two distinct compositional patterns, or classes of patterns: a general pattern, common to nonrodents and some rodents, and a murid pattern. (A third pattern, characterizing Megachiroptera, may also exist, but additional data are needed to confirm its existence.) Early studies of the compositional structures of mammalian genomes showed that the two murine genera *Mus* and *Rattus* had clear peculiarities compared to other commonly studied eutherians (Thiery *et al.*, 1976). Distinguishing characteristics of murine genomes include a different isochore organization (Cuny *et al.*, 1981; Salinas *et al.*, 1986), a narrower compositional distribution of coding sequences and third codon positions (Mouchiroud *et al.*, 1988; Bernardi, 1995), less stringent DNA repair and maintenance (see Holliday, 1995, and references therein), a faster rate of nucleotide substitution (Li and Tanimura, 1987; Chang *et al.*, 1994) and chromosomal rearrangements (Viegas-Pequignot *et al.*, 1986; Graves, 1996), and less pronounced or absent hypomethylated CpG islands (Aïssani and Bernardi, 1991a,b; Matsuo *et al.*, 1993; Antequera and Bird, 1993).

As the results presented here confirm with an enlarged data set, the CsCl profile of a species' total DNA suffices to determine the compositional pattern class (general or murid) to which it belongs. The profiles of Muridae (see Materials and Methods for the classification used here) can be recognized by their low skewness (asymmetry) and low percentage of very GC-rich ($\rho > 1.710$ g/cm^3), nonsatellite DNA. A third characteristic property suggested by previous results, namely high modal buoyant densities ($\rho_0 \geq 1.700$ g/cm^3), appears also to be shared by all Muridae. The fact that the Geomyoidea also exhibit high values of this parameter may be an artifact of unusually high proportions of satellite DNA, such as are found in other taxa of this superfamily (notably in kangaroo rats; see Hatch and Mazrimas, 1974). Alternatively, it may indicate high modal buoyant densities also of nonsatellite DNA in this superfamily, which McKenna and Bell (1972) include in the Myomorpha suborder together with the Muridae and the Gliridae.

The phylogeny of rodents is far from settled, as this group is remarkable for having gone through a rapid radiation leading to a tremendous diversity of fossil and recent taxa (Hartenberger, 1994, 1998a,b). Given the paucity of sequence data in many rodent families (but see Huchon *et al.*, 1999; Robinson *et al.*, 1997a, and references therein) and the rather large homoplasy of morphological data, an additional type of molecular character that could detect or confirm relationships among the higher taxa (families and above) would be a valuable tool. Given the diversity, yet relatively recent radiation, of rodents, this order appeared to be an ideal taxon in which to explore the uses of the CsCl profile as a contribution to taxonomy and eventually to phylogeny. We therefore obtained more species' profiles from a wide range of rodent families and, using this larger taxonomic sample, compared the groups of taxa that they imply with established or traditional phylogenies. We also wished to obtain a more precise picture of the two classes of compositional pattern within the rodent order and to determine whether the pattern of the murines is present in rodents other than Muroidea or Myomorpha.

In previous work (Thiery *et al.*, 1976; Macaya *et al.*, 1976; Salinas *et al.*, 1986; Sabeur *et al.*, 1993), CsCl profiles and/or compositional patterns were obtained for a total of 20 eutherian species spanning nine orders. The present study shows results of analytical centrifugation experiments in CsCl density gradients for 17 additional rodent species. Together with the 8 rodent species for which results were already available, the collection of rodent profiles now comprises 24 genera, representing 19 families of living rodents. Early rodent CsCl profiles that were published (Walker, 1968; Hennig and Walker, 1970; Mazrimas and Hatch, 1972) are unfortunately unreliable due to distortion vertically (nonlinear responses) and, for at least one data set, horizontally (nonmonotonous buoyant density scale); with the partial information that they contain, however, they would raise the number of profiled rodent genera to 31. Rodents encompass more than 2000 living species, or approximately 40% of all mammals (Wilson and Reeder, 1993). Since the taxon Rodentia includes several higher-level taxa, such as suborders (e.g., Sciuromorpha, Hystricognatha, and Myomorpha) and superfamilies (e.g., Muroidea, Cav-

ioidea, and Geomyoidea), care was taken to choose appropriate exemplars for representing parts of this speciose eutherian order. The measurements of the profiles obtained here show that rodents harbor a large diversity of modal buoyant densities spanning the entire scatter of values observed in other eutherians. This diversity led us to explore in further detail the variation of modal buoyant density and other CsCl profile parameters, especially measures of skewness, among rodent taxa of different levels.

MATERIALS AND METHODS

DNA Preparation

DNAs were extracted, using a procedure slightly modified from that of Kay *et al.* (1952), from ethanol-preserved tissue samples (in most cases from liver) in the Collection of Mammalian Tissues of Montpellier (Catzeflis, 1991). The 17 species were chosen to ensure wide sampling: the total number of species analyzed (previous studies and this study) represents over 60% of the rodent familial diversity and allows the extent of variation at different taxonomic levels to be assessed. Care was taken to obtain DNA extracts of the best quality. Molecular weights of the DNA fragments were shown to be >40 kb by electrophoresis on 0.2% agarose gel.

Taxonomy and Classification

Family and subfamily definitions mainly follow Wilson and Reeder (1993, pp. 7–8). For Muridae *sensu lato* we considered five subfamilial taxa: Cricetinae, Murinae, Arvicolinae, Spalacinae, and Sigmodontinae. For taxa above the family level, we mainly follow the recent synthesis of McKenna and Bell (1997); for convenience, the arrangement of the taxa studied here is summarized in Fig. 2. Alternative hypotheses and systematic arrangements are cited throughout the discussion.

CsCl Profiles

CsCl profiles of the extracted DNAs were obtained by analytical ultracentrifugation to sedimentation equilibrium in a CsCl gradient as previously described (Thiery *et al.*, 1976; Sabeur *et al.*, 1993). For conversion between buoyant density and GC level, the relation of Schildkraut *et al.* (1962) was used: $\rho = (\mathrm{GC} \times 0.098)/100 + 1.66$. This relation is valid for the genomes studied here, since methylation levels of all mammals studied are ≤1.4% (Jabbari *et al.*, 1997). Two previously studied species, *Mus musculus* and *Crocidura russula* (a shrew), were reanalyzed to compare our new set of experimental values with those of Sabeur *et al.* (1993). The modal buoyant densities that we found were very similar to those previously published (1.7007 vs 1.7006 and 1.6974 vs 1.6976 g/cm^3) and are within the experimental error, ±0.5 mg/cm^3 (Thiery *et al.*, 1976). For analysis of the profiles, each CsCl plot (from a Beckman Model E ultracentrifuge) was digitized at 64 points and normalized to unit area.

Curve Fitting

Estimating unknown compositional patterns from total DNA CsCl profiles by attempting a direct Gaussian decomposition is not robust, mainly because cryptic satellites can be present. A total of 8–15 parameters are needed to specify the major components of mammalian genomes, so that "false positive" fits would be frequent in the absence of additional information, such as the profiles of compositional fractions (see, e.g., Macaya *et al.*, 1976; Zoubak *et al.*, 1996). CsCl profiles were therefore not fitted by sums of Gaussians, but by functions that had succeeded in approximating or sketching, using only two parameters, the overall shapes of most vertebrate compositional patterns obtained so far. Such patterns typically show a roughly exponential decrease in the amount of DNA from the GC-poorest to the GC-richest component. We therefore fitted the CsCl profile (main band) to a truncated exponential curve of rate k, truncation point (highest value) ρ_c, and area A, that had been broadened by convolution with a Gaussian spread function of variance σ^2 and unit area. The fits are shown together with the profiles in Fig. 1. In the limit of no skewness, a truncated exponential becomes a sharp peak ($1/k \rightarrow 0$); so, the fit function becomes a Gaussian. In the limit of no broadening ($\sigma \rightarrow 0$), the fit function rises vertically from zero to its maximum value at ρ_c and then descends exponentially. In all other cases of positive skewness, the truncation point of the underlying exponential, ρ_c, will be to the left of the profile's peak or mode, ρ_0, which will in turn be to the left of the profile's mean, $\langle\rho\rangle$. Thus, increasing the symmetrical broadening σ, e.g., by choosing low-molecular-weight DNA (and so allowing increased diffusion of DNA in the ultracentrifuge cell), will shift the mode ρ_0 to the right (higher values), consistent with experimental results (see Thiery *et al.*, 1976; Macaya *et al.*, 1976). Further details on the truncated exponential curve and convolutions can be found in Bracewell (1986).

Standard numerical deconvolution techniques are not robust (Roe, 1992; Press *et al.*, 1988; and our pilot studies), but for this particular fit function $f(\rho)$ the convolution integral can be evaluated analytically, yielding an exact formula,

$$f(\rho) = A\ k\ \exp(k(\rho_c - \rho) + k^2\sigma^2/2)\Phi((\rho - \rho_c)/\sigma - k\sigma),$$

where Φ is the standard cumulative Gaussian distribution. This fit function has mean $\rho_c + 1/k$, variance $1/k^2 + \sigma^2$, and third moment $2/k^3$; the percentage of fitted (nonsatellite) DNA with $\rho > \rho_1 = 1.710$ g/cm^3 is approximately $\exp(k(\rho_c - \rho_1) + k^2\sigma^2/2) \times 100\%$.

Automated fitting requires modifying the usual sum of squares criterion, encouraging fits to pass below

(bypassing satellites) rather than above the CsCl profile and giving a higher weight to important regions in which data points are sparse (such as the steep rise on the left side of the profile and the peak region); these modifications still require fine tuning and testing. For the present study, we fitted the CsCl profiles by simple manual tuning of parameters and by visual inspection of fit and residuals. A consistency check for the parameters obtained was then given by the independent measurements of the samples' molecular weights: of the 17 species analyzed, the 4 species with the widest spread functions, as determined by the best fits, included as expected the 2 species with lowest molecular weight samples (*Ctenodactylus vali* and *Oecomys paricola*). The fits to most CsCl profiles were satisfactory (shown in Fig. 1), except for the two Geomyoidea profiles, as a result of particularly cryptic satellites. Two skewness parameters were used in this study, $\langle\rho\rangle - \rho_0$ and $1/k$. The latter parameter is one of the intrinsic fit parameters and thus avoids mode estimation errors and satellite contributions; furthermore, it also allows the former parameter to be calculated indirectly, for the fit, since $\langle\rho\rangle = \rho_c + 1/k$ and $(\rho_0 - \rho_c)/\sigma - k\sigma$ is the solution of $k\sigma\Phi(x) = \phi(x)$, where $\phi(x)$ is the standard Gaussian function (noncumulative distribution). By construction, the fit function allows the parameters $1/k$ and ρ_c to be largely independent of molecular weight and satellites, since σ should filter out most of the molecular weight dependence, and the form of the fit function should filter out satellites.

RESULTS AND DISCUSSION

Rodent Modal Buoyant Densities Span a Wide Range

The CsCl profiles obtained and used for this study are shown in Fig. 1, in order of increasing ρ_0. The profile of *Mus musculus*, previously investigated, was included as a calibration check. Also shown in the same plots are fits to broadened exponential distributions. These fit distributions are essentially characterized by two parameters: the rate of the underlying (unbroadened) exponential decrease, k, which is inversely related to the profile skewness, and the starting point of the exponential decrease, ρ_c, which is typically close to the buoyant density of the major component containing most DNA (see Materials and Methods and below).

The modal buoyant densities in CsCl, ρ_0, of all genomes investigated here are listed in Table 1, together with the values for previously studied rodent species. Measurements of modes from three early references (see legend to Table 1) are also given, in brackets. The values from these early sources will not be used further here, since they are only rough estimates obtained from published illustrations of CsCl curves and since the horizontal calibrations of some of the species' profiles are inconsistent.

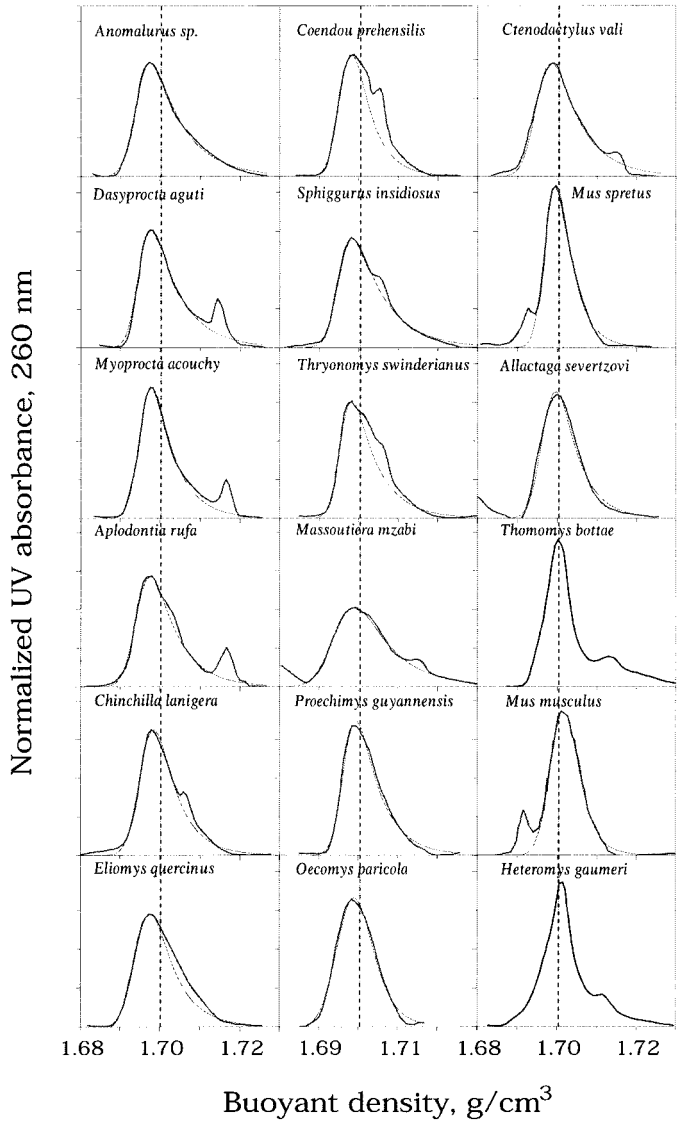

FIG. 1. CsCl profiles of 18 rodent species (bold line) and their best fits by broadened exponential distributions (thin dashed lines). The abscissa shows modal buoyant density in g/cm^3; the ordinate shows relative amounts of DNA. All profiles are normalized to unit area and shown in three columns in order of increasing modal buoyant density. No fits are shown for the two Geomyoidea profiles (see text). The dashed vertical line, at 1.7015 g/cm^3, indicates the mean buoyant density of the 18 species.

Figure 2 shows the range of rodent and other eutherian ρ_0 values in a graphical display. Above the family level, the taxa are grouped according to the systematic arrangement of McKenna and Bell (1997).

A comparison with the previously obtained values for other eutherians ($1.696 < \rho_0 < 1.701$; Fig. 2, bottom row) shows that rodent modal buoyant densities ($1.697 < \rho_0 < 1.701$) span practically the entire eutherian range: among nonrodents, only the very GC-poor fruit bat *Pteropus* sp. has a lower ρ_0 than the

TABLE 1

Modal Buoyant Densities and Other Parameters of Rodent DNAs as Determined by Analytical Centrifugation at Equilibrium in CsCl

Family	Subfamily	Species		Source	ρ_0 (g/cm^3)	$\langle\rho\rangle$ (g/cm^3)	$\langle\rho\rangle - \rho_0$ (mg/cm^3)	Higher taxa code	ρ_c (g/cm^3)	$1/k$ (mg/cm^3)	σ (mg/cm^3)
Dipodidae	Allactaginae	*Allactaga severtzovi*	Four-toed jerboa	a	1.7003	1.7016	1.3	MYO	1.69685	5.16	2.74
Muridae	Arvicolinae	*Clethrionomys glareolus*	Red-backed vole	d	[1.701]						
		Clethrionomys nageri/glareolus	Red-backed vole	d	[1.699]						
		Microtus agrestis	Meadow vole	d	[1.701]						
		Microtus/Chionomys nivalis	Snow vole	d	[1.701]						
		Arvicola amphibius/terrestris	Water vole/water rat	d	[Uncalibrated]						
	Murinae	*Mus musculus*	House mouse	a,b	1.7007	1.7012	0.5	MYO	1.69949	3.16	2.84
		Mus spretus	Algerian mouse	a	1.6996	1.7001	0.5	MYO	1.69744	3.87	2.25
		Rattus norvegicus	Brown rat	b	1.7008	1.7024	1.6	MYO			
		Rattus rattus	House rat	d	[1.703]						
		Acomys minous	African spiny mouse	d	[1.701]						
		Apodemus mystacinus	Field mouse	d	[1.700]						
		Apodemus sylvaticus	Field mouse	d	[1.700]						
		Apodemus flavicollis	Field mouse	d	[1.700]						
		Apodemus agrarius	Field mouse	d	[1.699]						
	Cricetinae	*Cricetulus* sp.	Hamster/dwarf hamster	b	1.7000	1.7021	2.1	MYO			
	Spalacinae	*Spalax* sp.	Blind mole-rat	b	1.7000	1.7019	1.9	MYO			
	Sigmodontinae	*Oecomys paricola**	Arboreal rice rat	a	1.6992	1.6998	0.6	MYO	1.69626	3.87	3.77
		Peromyscus maniculatus	Deer mouse	d	[1.700]						
Heteromyidae	Heteromyinae	*Heteromys gaumeri*	Spiny pocket mouse	a	1.7009	1.7027	1.8	GEO	—	—	—
	Dipodomyinae	*Dipodomys ordii*	Kangaroo rat	c	[1.703]						
		Dipodomys microps	Kangaroo rat	c	[1.702]						
		Dipodomys agilis	Kangaroo rat	c	[1.698]						
		Dipodomys panamintinus	Kangaroo rat	c	[1.698]						
		Dipodomys stephensi	Kangaroo rat	c	[1.698]						
		Dipodomys ingens	Kangaroo rat	c	[1.698]						
		Dipodomys heermanni	Kangaroo rat	c	[1.701]						
		Dipodomys merriami	Kangaroo rat	c	[1.698]						
		Dipodomys elator	Kangaroo rat	c	[1.698]						
		Dipodomys nitratoides	Kangaroo rat	c	[1.698]						
		Dipodomys spectabilis	Kangaroo rat	c	[1.700]						
		Dipodomys deserti	Kangaroo rat	c	[1.701]						
Geomyidae	—	*Thomomys bottae*	Pocket gopher	a	1.7006	1.7042	3.6	GEO	—	—	—
Gliridae (Myoxidae)	Glirinae (Myoxinae)	*Glis glis (Myoxinus glis)*	Fat dormouse	b	1.6991	1.7004	1.3	GLI			
	Leithiinae	*Eliomys quercinus*	Garden dormouse	a	1.6981	1.7005	2.4	GLI	1.69459	5.76	2.94
Sciuridae	Sciurinae	*Sciurus vulgaris*	Red squirrel	b	1.6982	1.7006	2.4	SCI			
		Marmota monax	Marmot/woodchuck	b	1.6983	1.7023	4.0	SCI			
Aplodontidae	—	*Aplodontia rufa*	Mountain beaver	a	1.6978	1.7016	3.8	APL	1.69459	6.32	2.74
Anomaluridae	Anomalurinae	*Anomalurus* sp.	Scaly-tailed squirrel	a	1.6974	1.7013	3.9	ANO	1.69429	7.78	2.74
Ctenodactylidae	—	*Ctenodactylus vali**	Thomas' gundi	a	1.6993	1.7016	2.3	HYS-	1.69518	7.10	2.89
		Massoutiera mzabi	Mzab gundi	a	1.6989	1.7031	4.2	HYS-	1.69459	8.91	4.21
Echimyidae	Eumysopinae	*Proechimys guyannensis*	Terrestrial spiny rat	a	1.6990	1.7017	2.7	HYS-	1.69665	5.90	2.45
Caviidae	Caviinae	*Cavia porcellus*	Guinea pig	b	1.6989	1.7018	2.9	HYS-			
Dasyproctidae (Agoutidae)	—	*Dasyprocta aguti/leporina*	(Red-rumped) agouti	a	1.6976	1.7023	4.7	DAS	1.69489	7.00	2.35
		Myoprocta acouchy	(Red) acouchy	a	1.6976	1.7017	4.1	DAS	1.69528	5.44	2.35
Thryonomyidae	—	*Thryonomys swinderianus*	Cane rat	a	1.6988	1.7018	3.0	HYS-	1.69561	6.32	2.22
Erethizontidae	—	*Coendou prehensilis*	Brazilian porcupine	a	1.6984	1.7011	2.7	HYS-	1.69569	4.67	2.51
		Sphiggurus insidiosus	Hairy dwarf porcupine	a	1.6984	1.7021	3.7	HYS-	1.69528	7.84	2.74
Chinchillidae	—	*Chinchilla lanigera*	Chinchilla	a	1.6980	1.7007	2.7	HYS-	1.69562	5.44	2.74

Note. Taxonomic content of families and subfamilies follows Wilson and Reeder (1993, pp. 7–8). Sources are denoted by a, the present study; b, Sabeur *et al.* (1993); c, Mazrimas and Hatch (1972); d, Walker (1968) and Hennig and Walker (1970). Modal buoyant densities from sources c and d are approximate only and are shown in brackets, since they were estimated from published pictures of smoothed CsCl profiles; means and other parameters could not be calculated from those profiles because of nonlinear responses (unreliable vertical scales). Three-letter abbreviations for higher taxon groups are, in alphabetical order, ANO, Anomaluridae; APL, Aplodontidae; DAS, Dasyproctidae; GEO, Geomyoidea; GLI, Gliridae; HYS-, Hystricognathi minus Dasyproctidae + Ctenodactylidae; MYO, Myodonta; SCI, Sciuridae. The two species with lower molecular weights are denoted by asterisks.

rodents analyzed so far, namely 1.6965 g/cm^3 (Sabeur *et al.*, 1993; other low values for Megachiroptera are given in Arrighi *et al.*, 1972). Three rodent families (Aplodontidae, Dasyproctidae, and Anomaluridae) exhibit ρ_0 values significantly lower than the previously known range for this order. Three nonmuroid families have as high, or higher, ρ_0 values than the muroid families: Dipodidae, also in the Myodonta infraorder,

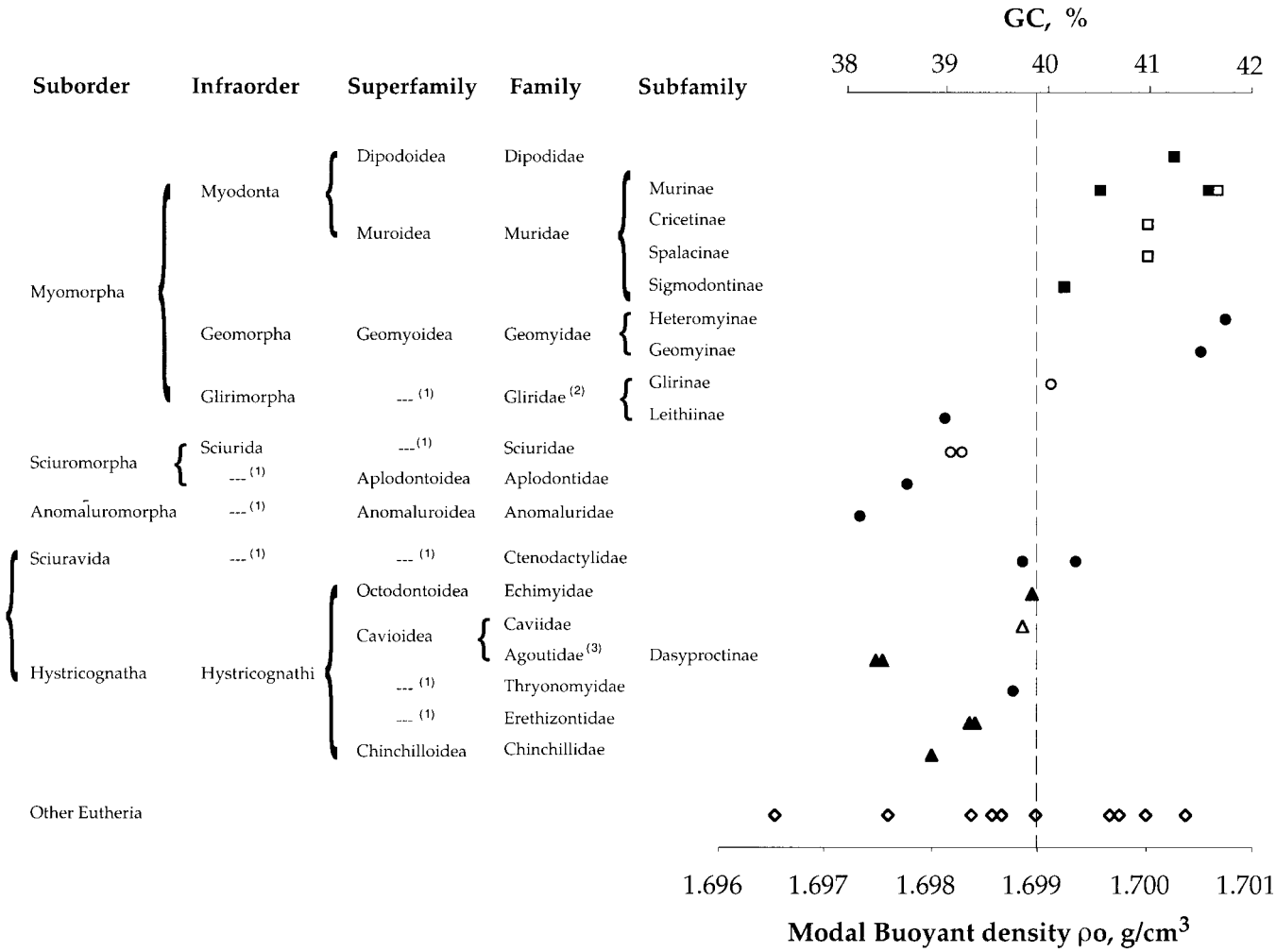

FIG. 2. Modal buoyant density and GC values of rodent and other eutherian DNAs. Closed and open symbols refer to our data and those of Sabeur *et al.* (1993), respectively. Triangles, squares, circles, and diamonds denote caviomorphs, muroids, other rodents, and other mammals, respectively. Each row shows the values grouped at the family or subfamily level. The systematic arrangement follows McKenna and Bell (1997). The grouping of the Ctenodactylidae (Sciuravida suborder) with the Hystricognatha suborder (leftmost bracket) is supported by results from nuclear DNA sequence comparisons (von Willebrand factor gene; Huchon *et al.*, 2000). For clarity, the two identical values observed in each of the Erethizontidae (1.6984 g/cm^3) and Dasyproctidae (1.6976 g/cm^3) have been artificially separated. With one exception (from Leithiinae), all the Myomorpha studied have modal buoyant densities $\rho_0 > 1.699$ g/cm^3 (dashed line); only one other rodent species (from Ctenodactylidae) has ρ_0 in this range. Other Eutheria are, from left to right: *Pteropus* sp. (megabat), *Crocidura russula* (shrew), *Homo sapiens* (man), *Felis domesticus* (cat), *Talpa europea* (mole), *Canis familiaris* (dog), *Manis* sp. (Asian pangolin), *Oryctolagus cuniculus* (rabbit), *Bos taurus* (cow), and *Erinaceus europaeus* (hedgehog). (1), Not named or not appropriate; (2), also called Myoxidae; (3), also called Dasyproctidae.

and Geomyidae and Heteromyidae, both in the Geomyoidea superfamily.

These results, obtained after improving the taxonomic diversity of the rodent CsCl profile collection, imply that the rodents cannot be distinguished from most other mammalian orders on the basis of modal buoyant density only. Similarly, this parameter alone also does not suffice to distinguish the muroid rodents (Spalacinae, Murinae, Sigmodontinae, and Cricetinae) from all other rodents, although all the species with high values similar to those of the muroids ($\rho_0 > 1.6994$) are in the same suborder, Myomorpha, in McKenna and Bell's (1997) classification (see Fig. 2). The wide modal buoyant density range for rodents suggests, moreover, that for many rodent taxa at the suborder, superfamily, and/or family levels, good resolution can be expected, exceeding experimental errors and the typical shifts in modes that can be caused by cryptic satellites. This prompted us to examine also other parameters that can be obtained from the rodent CsCl profiles (without directly estimating the nonrobust higher moments), to determine whether appropriate bivariate scatterplots could be used as maps to separate different rodent taxa.

Scatterplots Involving Pairs of Rodent CsCl Profile Parameters Can Separate Distant Taxa and Group Close Taxa

Mean, mode, and skewness. Figure 3 shows three scatterplots describing the rodent CsCl profiles with different parameters. In each panel the ordinate shows a skewness or asymmetry parameter. The first two panels (Figs. 3A and 3B) represent parameters calculated from the entire CsCl profile, without subtracting satellites that may be present in the main band. The third panel (Fig. 3C) represents parameters of the fit, which subtracts obvious satellites (see below, and Fig. 1). As the scatterplots show, the parameters allow the recognition of some families and higher-level taxa (e.g., Dasyproctidae, Myodonta, and Geomyoidea).

Figures 3A and 3B employ the mean buoyant density $\langle\rho\rangle$. The abscissa shows the modal buoyant density ρ_0 in Fig. 3A and $\langle\rho\rangle$ in Fig. 3B. In both plots, the ordinate shows the difference mean − mode ($\langle\rho\rangle - \rho_0$). This difference spans a range comparable to that observed for all vertebrates analyzed so far, namely from values near 0 to almost 5 mg/cm^3. In rodents other than the Myodonta (and one of the Geomyoidea), the values are in the range of other eutherians and birds (>2 mg/cm^3; Sabeur *et al.*, 1993; Thiery *et al.*, 1976). In contrast, the Myodonta attain the lower skewness values (nearly symmetric CsCl profiles) that are characteristic of cold-blooded vertebrates (Bernardi and Bernardi, 1990a,b). In this context, it should be added that Myodonta can be quickly distinguished from cold-blooded vertebrates using other profile parameters, such as the total heterogeneity (standard deviation, second moment). The latter parameter was not employed in the present study, however, since it is more sensitive to flanking satellite DNA and baseline shifts than the parameters used here, when calculated directly from the CsCl data; when calculated indirectly from the fit, it is a simple function of the fit parameters ($\sqrt{(1/k^2 + \sigma^2)}$; see below and Materials and Methods) and does not add new information.

Although the possible errors in estimating the mode ρ_0 or the mean $\langle\rho\rangle$ may amount to ±0.5 mg/cm^3 (Thiery *et al.*, 1976), the errors for the ordinates of Figs. 3A and 3B are less, since most errors are due to shifts of the entire profile along the modal buoyant density axis and vanish when we take the difference $\langle\rho\rangle - \rho_0$.

Three main taxa above the family level can be immediately recognized in Figs. 3A and 3B. The two representatives of the Geomyoidea superfamily, namely the pocket gopher *Thomomys* (Geomyidae) and the pocket mouse *Heteromys* (Heteromyidae), differ from the other rodents by their high mean GC. A second group that can be clearly distinguished comprises the represented Muridae and Dipodidae, i.e., the Myodonta of McKenna and Bell (1997). As far as the Gliridae are concerned, one genus, *Eliomys*, merges with

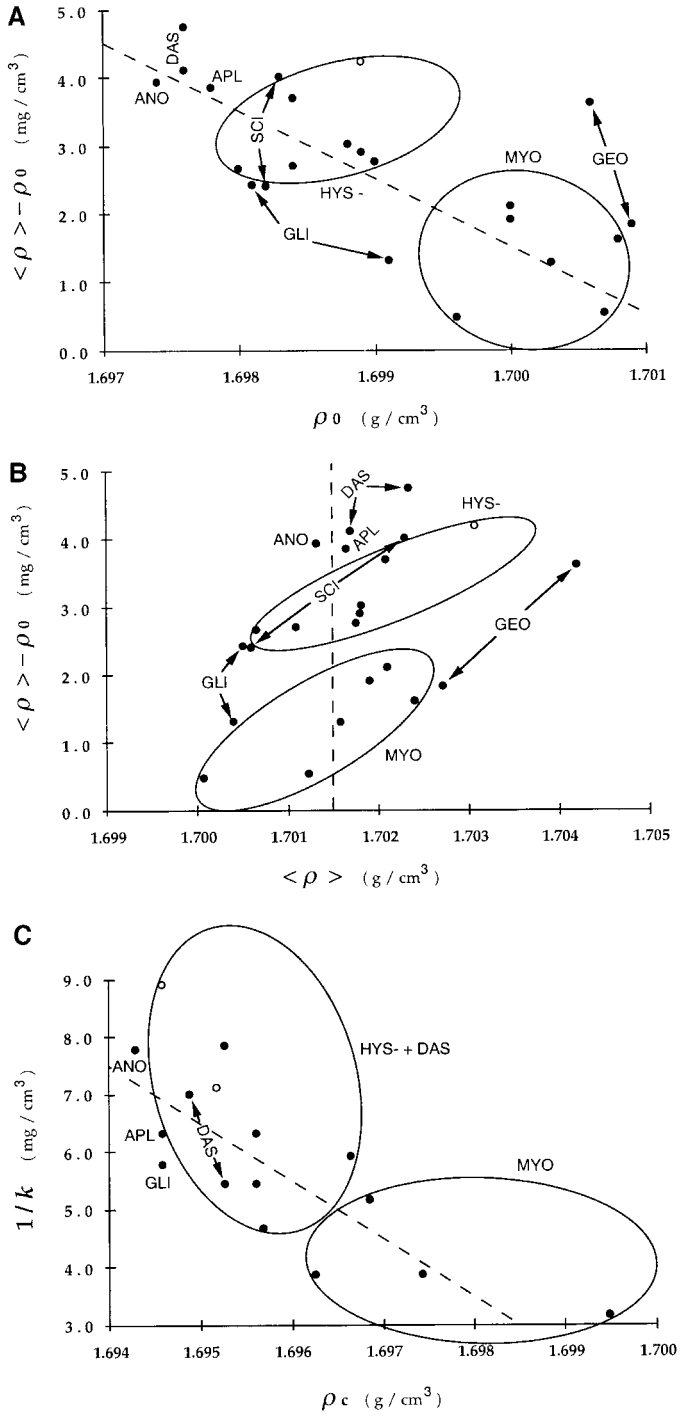

FIG. 3. Scatterplots showing skewness parameters ($\langle\rho\rangle - \rho_0$ and $1/k$; ordinate) and other parameters (ρ_0, $\langle\rho\rangle$, ρ_c; abscissa) of rodent CsCl profiles of total nuclear DNA. Dashed lines in (A) and (C) indicate where the points would be found if the mean buoyant densities of all species' profiles (or of their fits, in C) were identical, at 1.7015 g/cm^3 (see text). Ctenodactylidae are indicated by open circles. The ellipses are used only to indicate groups of points, not domains or limits for the taxa in question. Parameter values shown in the scatterplots, and three-letter abbreviations for higher taxa, are as in Table 1. Two species (*Oecomys paricola* and *Ctenodactylus vali*) are not shown in (A) and (B) because of the samples' lower molecular weights. In (C), only profiles obtained and fitted in the present study are represented.

species that are phylogenetically distant from the Myomorpha, whereas the other, *Glis,* is located closer to the Myodonta, but not necessarily among them, on the plots; for both Gliridae a lower modal buoyant density is the distinguishing feature. A third group consists of the Hystricognathi + Ctenodactylidae, with the exception of the family Dasyproctidae; this apparent separation into two groups is, however, not robust (see below and Fig. 3C, where the taxa in question form a single group).

We checked the similarity of the CsCl parameters in different genera of the same family and in two different species within the same genus (*Mus*). The two Dasyproctidae remain close together on all plots of Fig. 3, and their profiles are also qualitatively similar, with similar shapes and a bump (apparently satellite DNA) at 1.715–1.717 g/cm^3. The same is true for the two Erethizontidae. The two species within the Gliridae (see above) have similar means but different modes (Fig. 3A), whereas those within the Sciuridae have similar modes but different means (Fig. 3B). Finally, the two *Mus* species have as a common parameter the near symmetry of their profiles (very low $\langle\rho\rangle - \rho_0$), although their means and modes differ considerably, by 0.01 g/cm^3.

Interestingly, the parameters and shape of the *Aplodontia* CsCl profile, including a bump at 1.715–1.717 g/cm^3, show a strong similarity to those of the two Dasyproctidae. Parameters similar to those of these three species are shown also by one (*Marmota*) of the two divergent representatives of Sciuridae and by the single Anomaluromorpha. Aplodontidae and Sciuridae are the only living families of the suborder Sciuromorpha, and their proximity is also sustained by molecular phylogenetics (Nedbal *et al.,* 1996; Huchon *et al.,* 1999). Whereas Dasyproctidae is an advanced family of Caviomorpha, corresponding to the Caviida of McKenna and Bell (1997) plus the Erethizontidae, the scaly-tailed flying squirrel (Anomaluridae) represents a divergent suborder (Anomaluromorpha).

Of upmost interest is the proximity of the two Ctenodactylidae (cf. also Fig. 3C) to most of the Hystricognathi, since the evolutionary systematics of gundis (Ctenodactylidae) has long been an enigma. It has been proposed that they should be placed in their own suborder (Sciuravida; McKenna and Bell, 1997), that they are *incertae sedis* (with Hystricomorpha or with Myomorpha; Simpson, 1945), or that they are the sister group of the Hystricognathi (Bryant and McKenna, 1996). The molecular data obtained so far have been inconclusive: gundis have appeared either as the sister clade of Sciuroidea, when mitochondrial 12S ribosomal RNA sequences were compared (Nedbal *et al.,* 1997), or, together with the Hystricognathi, as an early offshoot of the order Rodentia, when nuclear (globin) protein sequences were analyzed (Beintema *et al.,* 1991). The available CsCl profiles, as well as a recent nuclear (vWF) sequence comparison (Huchon *et al.,* 2000), group Ctenodactylidae with Hystricognathi rather than with Sciuroidea, Gliroidea, or Myodonta.

Cryptic satellite DNA in CsCl profiles can confound phylogenetic inference. At first sight, the profiles of the two genera from the Geomyoidea superfamily shown in Fig. 1 (*Thomomys* and *Heteromys*) appear to be mirror images of typical CsCl profiles, i.e., similar to the profiles of other rodents but with negatively (left) skewed main bands. That this is an artifact is suggested by the observation that all other vertebrate profiles obtained to date, including 120 species of fish, are positively (right) skewed, except for a few fish species in which cryptic satellite DNA causes an apparent negative skew (Bernardi and Bernardi, 1990a,b). This suspicion is supported further by the record percentages (over 50%) of satellite DNA that have been found in some, although not all, species of the kangaroo rat genus *Dipodomys,* which are in the same family as *Heteromys* (Heteromyidae) (Mazrimas and Hatch, 1972; Hatch and Mazrimas, 1974; Hatch *et al.,* 1976); the buoyant density of some of this satellite DNA is close to the modes of *Thomomys* and *Heteromys.* The unusual shape of the two Geomyoidea profiles is thus probably caused by large amounts of cryptic satellite DNA near the mode. The pocket gopher genus *Thomomys* represented here exhibits some of the most atypical recombinational behavior and karyotypic diversity known in mammals, including wide differences in chromosome configuration among local populations of the same species (Patton, 1972; Patton and Yang, 1977), low gene flow, and low number of chiasmata per bivalent when age to maturity is taken into account (Burt and Bell, 1987). Similar extreme inter- and intraspecific diversities in satellite and heterochromatin content or karyotype have been observed also in other Geomyoidea genera (e.g., in the pocket mouse *Perognathus goldmani;* Patton, 1969). These observations indicate that the profile characterization problems encountered here in the case of Geomyoidea are likely to be among the most extreme that can occur in mammals.

Satellite DNA is often found, as its name implies, in separate, narrow bands or modes located at a certain distance from the main band or from its main mode. In some species, however, so-called "cryptic satellites" exist that are hidden within the main band. Satellite DNA can, as an artifact, either downplay or exaggerate CsCl profile differences that would otherwise be informative. For example, shifts in $\langle\rho\rangle$, ρ_0, or $\langle\rho\rangle - \rho_0$ that occur between closely related taxa are sometimes due only to satellite DNA differences. When such satellite differences occur at the family level or higher, their effect is similar to a measurement error. Measurements of the mode ρ_0 depend sensitively on any cryptic satellites that may be present near it on the buoyant

density axis, whereas measurements of the mean $\langle\rho\rangle$ depend sensitively on satellites (and on any baseline inaccuracies) that may be present far from it. A GC-poor satellite peak, as occurs for example in the mouse profiles, can shift the mean to the left without affecting the mode, thus decreasing the skewness parameter $\langle\rho\rangle - \rho_0$.

The sensitivity to satellites of the traditional CsCl profile parameters, and, to a lesser extent, their dependence on molecular weight, prompted us to look for alternative parameters that are phylogenetically more robust, at the level of higher taxa. The new parameters presented here, namely those specifying a broadened exponential fit (k, ρ_c, and σ; see Materials and Methods) that bypasses obvious satellites, represent a first step in this direction.

The choice of our fit function was based on the assumption, valid in all vertebrate profiles for which satellite analyses are available to date, that narrow bumps deviating significantly from the typical smooth CsCl profile shapes are due to satellite DNA. For example, the guinea pig's main band is bimodal, but one of the modes is due to a bump of narrow width that has been shown to be due to satellite DNA (Sabeur *et al.*, 1993; cf. also Corneo *et al.*, 1968) and that does not, therefore, represent DNA containing genes.

Fit parameters. Figure 3C shows a scatterplot employing the two main parameters of the fits, for the 18 species whose profiles were obtained in this study: the skewness parameter, $1/k$, and the peak buoyant density of the underlying exponential function, ρ_c. Since k describes the rate of the exponential fit, $1/k$ measures skewness and vanishes when the profile is symmetric. By construction of the (unimodal) fit, this scatterplot discounts obvious satellites and can thus reveal phylogenetically relevant information that is hidden in Figs. 3A and 3B, such as the proximity of the Dasyproctidae to the other Hystricognathi. It also allows comparison of species represented by samples of different molecular weight, such as the two Ctenodactylidae, since most molecular weight differences are absorbed by the spread parameter σ.

The scatterplots in Fig. 3 suggested the presence of correlations, e.g., a negative correlation between skewness and modal buoyant density among the rodents. These correlations, which were confirmed as significant with good regression coefficients (not shown here), are largely a trivial consequence of the low diversity of rodents' mean buoyant densities, especially after discounting satellites, compared to the wide range of their modal buoyant densities. Indeed, mean GC values of the fits (calculated using $\langle\rho\rangle = \rho_c + 1/k$; see Materials and Methods) have a mean at 42.3% GC and a SD of only 1.2%, for the 18 rodent species analyzed here. A narrow range of mean GC values is found not only for rodents, but for eutherians in general (see Jabbari *et al.*, 1997 for a table of vertebrates' mean GC levels). Dashed lines in Fig. 3 show, as a reference, the lines on which the points would lie if mean GC values of all species were identical at 42.3% GC ($\langle\rho\rangle = 1.7015$ g/cm^3). The correlation(s) can also be seen by tracking the position of the mode as one looks at the successive plots of Fig. 1, which are presented in order of increasing modal buoyant density. Roughly, the skew of the main band DNA is positive and highest for species having low modal buoyant density, it decreases as the mode increases, it passes through 0 (perfect symmetry) when the mode reaches a value around 1.7005–1.7015 g/cm^3, and it appears to becomes negative when the mode exceeds this value.

Very GC-rich DNA

When comparing CsCl profiles from different taxa, it is important to visualize where the genes are located. For example, in the GC-richest, gene-richest isochore family of the human genome, H3, gene densities are around 17–20 times higher than those in the GC-poor families L1 and L2 (Mouchiroud *et al.*, 1991; Zoubak *et al.*, 1996). The distribution of genes found in human is similar to those in other nonrodent mammals, whereas the murids so far studied are characterized by reduced CsCl profile (main band) skewness, a relative absence of very GC-rich DNA having $\rho > 1.710$ g/cm^3, and a shift of the GC-richest genes toward GC-poorer DNA, called the *minor shift* (see Bernardi *et al.*, 1995 and references therein). This compositional shift of genes can be seen as a shift in slot blot hybridization patterns: the GC-richest gene-containing DNA of rodents, which can be identified by hybridization with the GC-richest gene-containing DNA of human (H3), is located in GC-rich fractions in squirrel and guinea pig (non-Muridae), but in GC-poorer fractions in mouse and mole rat (Muridae) (Cacciò *et al.*, 1994).

The new profiles apparently also confirm a criterion for Muridae that was suggested by the results of Sabeur *et al.* (1993), namely low percentages of very GC-rich, nonsatellite DNA having $\rho > 1.710$ g/cm^3. For the CsCl profiles in which the fits of Fig. 1 correspond well to the nonsatellite DNA, the percentage of this very GC-rich DNA can be estimated (see Materials and Methods). Although such estimates become very rough as soon as a genome contains GC-rich satellites, even when the CsCl profiles of compositional fractions are available (as pointed out already in Sabeur *et al.*, 1993), and especially in the absence of such data, the new profiles obtained apparently confirm this working criterion. In the Muridae, estimates of the percentage of nonsatellite DNA with $\rho_0 > 1.710$ g/cm^3 remained below 6%; in all but one of the non-Muridae whose fits are shown in Fig. 1, they were above 6%. The apparent exception, *Coendou prehensilis*, may be due to cryptic satellite DNA in this species' main band causing a less reliable fit and therefore a less reliable estimate of the

percentage of very GC-rich DNA (5–6%). Estimates that were only slightly above 6% (between 7 and 9%) were obtained for the Dasyproctidae and the Gliridae studied here and for *Chinchilla*.

Origin of Some Special Phenomena Observed in the Murid Lineage

The reduced compositional contrasts that have been observed in the Muridae genomes, which concern both coding and noncoding DNA (see Introduction), are in all likelihood a consequence of the less meticulous repair and maintenance mechanisms that have been documented for these species, in particular for mouse and rat. Unless selection were more stringent in the Muridae than in other mammals, one would expect the reduction in accuracy of DNA synthesis, repair, and other genome maintenance activities observed in mouse and rat (cf. Holliday, 1995) to increase not only the mutation rate of individual cells, but also the rate at which mutations become fixed in the species, i.e., the substitution rate. Such higher substitution rates in mouse or rat compared to human have indeed been reported (see Li, 1997, and references therein; but cf. also Janke *et al.*, 1994). These increased substitution rates would, in turn, reduce the compositional heterogeneity and skewness of the affected genomes by randomizing base composition, thus shifting the mode of the buoyant density toward the mean, i.e., toward higher values. Such changes in the genomic GC distribution (CsCl profile) are indeed what one observes in the case of mouse, rat, and the other Myodonta studied (Figs. 2 and 3).

Since increased substitution rates are often loosely referred to as a property of rodents in general, without corresponding evidence, it seems worth pointing out that such generalization may be inappropriate. In fact, the results presented above strongly suggest that only certain myomorph rodents have been affected by increased substitution rates. This property and related properties such as lower genic or intergenic compositional contrasts or less-pronounced CpG islands (see Introduction) partition the rodent taxa into two groups. The group including mouse and rat appears to comprise the Myodonta infraorder and may include the entire Myomorpha suborder. If the CsCl profile data presented here can be used to parametrize the special properties of mouse and rat, as the available evidence indicates, then we would expect the division of rodents into two groups to have occurred after the lineage leading to the present Myomorpha separated from the other lineage(s) and at the latest shortly after the Myodonta lineage separated from the Glirimorpha and/or Geomorpha lineage(s).

Different substitution rates among rodent families have been observed also in phylogenetic analyses of nuclear DNA sequences (Huchon *et al.*, 1999, 2000), although high rates were reported also for several nonmyomorph taxa. Additional studies will be needed to delineate more precisely which rodents have been affected by high substitution rates and to what extent base compositional changes are correlated with them.

Do the Gliridae Belong to the Myomorpha?

An example in which CsCl profile comparisons may shed light on a century-old question in rodent phylogeny is given by the Gliridae: it has been much debated whether this family should be included among the Myomorpha, i.e., grouped with superfamilies such as Muroidea and Dipodoidea. Whereas for Simpson (1945), a suborder Myomorpha included Muroidea, Gliroidea, and Dipodoidea, McKenna and Bell (1997) have extended this view by recognizing three infraorders (Myodonta, Glirimorpha, Geomorpha) within the suborder Myomorpha. That Gliridae should not be included among the Myomorpha is suggested by morphological evidence, brought by Vianey-Liaud (1985), that would exclude dormice from the Myomorpha. Subsequently, Gliridae have been clustered with Sciuroidea on the basis of morphological (Bugge, 1985; Lavocat and Parent, 1985) and molecular (Huchon *et al.*, 1999) analysis. A comparison of mitochondrial genomes that includes the recently sequenced dormouse (Reyes *et al.*, 1998) is consistent with such views. The CsCl buoyant densities presented here locate both taxa of Gliridae in between Myodonta on the one hand and Hystricognathi + Ctenodactylidae on the other hand. As mentioned before, the garden dormouse *Eliomys* has some proximity with one Sciuroidea (*Sciurus*), whereas the fat dormouse *Glis* is located near the Myodonta. Thus, our results are ambiguous, and additional taxa of Gliridae, Dipodidae, and Sciuridae are needed for further inferences.

CONCLUSION

The results presented here show that mammalian CsCl profiles can directly yield phylogenetically relevant parameters. When rodent taxa were represented in scatterplots using pairs of such CsCl parameters, they formed groups on the scatterplot that corresponded largely to established rodent systematics, and most of the exceptions corresponded to taxa whose systematics are still under debate. CsCl profile analysis is, therefore, a DNA analysis that should compare favorably with DNA sequencing and traditional morphological analysis (e.g., of cranial or dental traits), as a way of quickly screening the genomes of many species for phylogenetic information. The rodent analyses presented here also suggest that the percentage of satellite DNA in a species' genome does not need to be measured separately, except possibly when this percentage attains very high levels, as in the case of certain Geomyoidea. Thus, once appropriate tissues have

been collected and properly conserved, the informative parameters can be rapidly obtained.

ACKNOWLEDGMENTS

This study would not have been possible without the generous help of all people who collected mammals in the field and preserved their valuable tissues. We thank P. Gambarian (*Allactaga*), J.-C. Gautun (*Anomalurus*), P. Gouat (Ctenodactylidae), V. Laudet (*Chinchilla*), D. Nolte (*Aplodontia*), J. L. Patton (*Thomomys*), T. Robinson (*Thryonomys*), and J.-C. Vie (Erethizontidae and Dasyproctidae). We also thank J. C. Aufray for help in digitizing the CsCl profiles, G. Macaya for helpful discussions, and G. Knott for e-mail correspondence on automatic curve-fitting. Laboratory experiments were funded by ACC-SV3 (grant to the network of D. Mouchiroud) and ACC-SV7 (Réseau National Biosystématique). Laboratory and theoretical work was funded also by a grant from the European Community (FRMX-CT98-0221 TMR/Network on Mammalian Phylogeny).

REFERENCES

Aïssani, B., and Bernardi, G. (1991a). CpG islands, genes and isochores in the genome of vertebrates. *Gene* **106:** 185–195.

Aïssani, B., and Bernardi, G. (1991b). CpG islands: Features and distribution in the genome of vertebrates. *Gene* **106:** 173–183.

Antequera, F., and Bird, A. (1993). Number of CpG islands and genes in human and mouse. *Proc. Natl. Acad. Sci. USA* **90:** 11995–11999.

Arrighi, F. E., Lidicker, W. Z., Mandel, M., and Bergendahl, J. (1972). Heterogeneity in CsCl buoyant densities of Chiropteran DNA. *Biochem. Syst.* **6:** 27–30.

Beintema, J. J., Rodewald, K., Braunitzer, G., Czelusniak, J., and Goodman, M. (1991). Studies on the phylogenetic position of the Ctenodactylidae (Rodentia). *Mol. Biol. Evol.* **8:** 151–154.

Bernardi, G., Olofsson, B., Filipski, J., Zerial, M., Salinas, J., Cuny, G., Meunier-Rotival, M., and Rodier, F. (1985). The mosaic genome of warm-blooded vertebrates. *Science* **228:** 953–958.

Bernardi, G. (1995). The human genome: Organization and evolutionary history. *Annu. Rev. Genet.* **29:** 445–476.

Bernardi, G. (2000). Isochores and the evolutionary genomics of vertebrates. *Gene* **241:** 3–17.

Bernardi, G., and Bernardi, G. (1990a). Compositional patterns in the nuclear genomes of cold-blooded vertebrates. *J. Mol. Evol.* **31:** 265–281.

Bernardi, G., and Bernardi, G. (1990b). Compositional transitions in the nuclear genomes of cold-blooded vertebrates. *J. Mol. Evol.* **31:** 282–293.

Bracewell, R. N. (1986). "The Fourier Transform and Its Applications," 2nd ed., McGraw–Hill, Boston.

Bugge, J. (1985). Systematic value of the carotid arterial pattern in rodents. *In* "Evolutionary Relationships among Rodents" (W. P. Luckett and J.-L. Hartenberger, Eds.), pp. 381–402. Plenum, New York.

Burt, A., and Bell, G. (1987). Mammalian chiasma frequencies as a test of two theories of recombination. *Nature* **326:** 803–805.

Cacciò, S., Perani, P., Saccone, S., Kadi, F., and Bernardi, G. (1994). Single-copy sequence homology among the GC-richest isochores of the genomes from warm-blooded vertebrates. *J. Mol. Evol.* **39:** 331–339.

Catzeflis, F. (1991). Animal tissue collections for molecular genetics and systematics. *Trends Ecol. Evol.* **6:** 168.

Chang, B. H.-J., Shimmin, L. C., Shyue, S.-K., Hewett-Emmett, D., and Li, W.-H. (1994). Weak male-driven molecular evolution in rodents. *Proc. Natl. Acad. Sci. USA* **91:** 827–831.

Corneo, G., Ginelli, E., Soave, C., and Bernardi, G. (1968). Isolation and characterization of mouse and guinea pig satellite DNAs. *Biochemistry* **7:** 4373–4379.

Cuny, G., Soriano, P., Macaya, G., and Bernardi, G. (1981). The major components of the mouse and human genomes. I. Preparation, basic properties and compositional heterogeneity. *Eur. J. Biochem.* **115:** 227–233.

Graves, J. A. M. (1996). Mammals that break the rules: Genetics of marsupials and monotremes. *Annu. Rev. Genet.* **30:** 233–260.

Hartenberger, J.-L. (1994). The evolution of the Gliroidea. *In* "Rodent and Lagomorph Families of Asian Origins and Diversification" (Y. Tomida, C. K. Li, and T. Setoguchi, Eds.), Vol. 8, pp. 19–33. National Science Museum Monographs, Tokyo.

Hartenberger, J.-L. (1998a). The Cenozoic radiation of mammals: Some comments on the shape and tempo of a major evolutionary event. *Paleontol. Lombardia* **8:** 3–21.

Hartenberger, J.-L. (1998b). Description de la radiation des Rodentia (Mammalia) du Paléocène supérieur au Miocène; incidences phylogénétiques. *C. R. Acad. Sci. Paris* **326:** 439–444.

Hatch, F. T., and Mazrimas, J. A. (1974). Fractionation and characterization of satellite DNAs of the kangaroo rat (*Dipodomys ordii*). *Nucleic Acids Res.* **1:** 559–575.

Hatch, F. T., Bodner, A. J., Mazrimas, J. A., and Moore, D. H. II. (1976). Satellite DNA and cytogenetic evolution: DNA quantity, satellite DNA and karyotypic variations in kangaroo rats (genus *Dipodomys*). *Chromosoma* **58:** 155–168.

Hennig, W., and Walker, P. M. B. (1970). Variations in the DNA from two rodent families (Cricetidae and Muridae). *Nature* **225:** 915–919.

Holliday, R. (1995). "Understanding Ageing," Cambridge Univ. Press, Cambridge.

Huchon, D., Catzeflis, F. M., and Douzery, E. J. P. (1999). Molecular evolution of the nuclear von Willebrand factor gene in mammals and the phylogeny of rodents. *Mol. Biol. Evol.* **16:** 577–589.

Huchon, D., Catzeflis, F. M., and Douzery, E. J. P. (2000). Variance of molecular datings, evolution of rodents and the phylogenetic affinities between Ctenodactylidae and Hystricognathi. *Proc. R. Soc. Lond. B,* **267:** 393–402.

Jabbari, K., Cacciò, S., Païs de Barros, J. P., Desgrès, J., and Bernardi, G. (1997). Evolutionary changes in CpG and methylation levels in the genome of vertebrates. *Gene* **205:** 109–118.

Janke, A., Feldmaier-Fuchs, G., Thomas, W., von Haeseler, A., and Pääbo, S. (1994). The marsupial mitochondrial genome and the evolution of placental mammals. *Genetics* **137:** 243–256.

Kay, E. R. M., Simmons, N. S., and Dounce, A. L. (1952). An improved preparation of sodium desoxyribonucleate. *J. Am. Chem. Soc.* **74:** 1724–1726.

Lavocat, R., and Parent, J.-P. (1985). Phylogenetic analyses of middle ear features in fossil and living rodents. *In* "Evolutionary Relationships among Rodents" (W. P. Luckett and J.-L. Hartenberger, Eds.), pp. 333–354. Plenum, New York.

Li, W.-H. (1997). "Molecular Evolution," Sinauer, Sunderland, MA.

Li, W.-H., and Tanimura, M. (1987). The molecular clock runs more slowly in man than in apes and monkeys. *Nature* **326:** 93–96.

Macaya, G., Thiery, J. P., and Bernardi, G. (1976). An approach to the organization of eukaryotic genomes at a macromolecular level. *J. Mol. Biol.* **108:** 237–254.

Matsuo, K., Clay, O., Takahashi, T., Silke, J., and Schaffner, W. (1993). Evidence for erosion of mouse CpG islands during mammalian evolution. *Somat. Cell Mol. Genet.* **19:** 543–555.

Mazrimas, J. A., and Hatch, F. T. (1972). A possible relationship between satellite DNA and the evolution of kangaroo rat species (genus *Dipodomys*). *Nature New Biol.* **240:** 102–105.

McKenna, M. C., and Bell, S. K. (1997). "Classification of Mammals above the Species Level," Columbia Univ. Press, New York.

Mouchiroud, D., Gautier, C., and Bernardi, G. (1988). The compositions distribution of coding sequences and DNA molecules in humans and murids. *J. Mol. Evol.* **27:** 311–320.

Mouchiroud, D., D'Onofrio, G., Aïssani, B., Macaya, G., Gautier, C., and Bernardi, G. (1991). The distribution of genes in the human genome. *Gene* **100:** 181–187.

Nedbal, M. A., Honeycutt, R. L., and Schlitter, D. A. (1996). Higher level systematics of rodents (Mammalia, Rodentia): Evidence from the mitochondrial 12S gene. *J. Mammal. Evol.* **3:** 201–237.

Patton, J. L. (1969). Chromosome evolution in the pocket mouse *Perognathus goldmani* Osgood. *Evolution* **23:** 645–662.

Patton, J. L. (1972). Patterns of geographic variation in karyotype in the pocket gopher, *Thomomys bottae* (Eydoux and Gervais). *Evolution* **20:** 574–586.

Patton, J. L., and Yang, S. Y. (1977). Genetic variation in *Thomomys bottae* pocket gophers: Macrogeographic patterns. *Evolution* **31:** 697–720.

Pettigrew, J. D., and Kirsch, J. A. W. (1995). Flying primates revisited: DNA hybridization with fractionated, GC-enriched DNA. *S. Afr. J. Sci.* **91:** 477–482.

Press, W. H., Flannery, B. P., Teukolsky, S. A., and Vetterling, W. T. (1988). "Numerical Recipes in C: The Art of Scientific Computing," pp. 425–431, Cambridge Univ. Press, Cambridge.

Reyes, A., Pesole, G., and Saccone, C. (1998). Complete mitochondrial DNA sequence of the fat dormouse, *Glis glis:* Further evidence of rodent paraphyly. *Mol. Biol. Evol.* **15:** 499–505.

Robinson, M., Catzeflis, F., Briolay, J., and Mouchiroud, D. (1997a). Molecular phylogeny of rodents, with special emphasis on Murids: Evidence from nuclear gene LCAT. *Mol. Phylogenet. Evol.* **8:** 423–434.

Robinson, M., Gautier, C., and Mouchiroud, D. (1997b). Evolution of isochores in rodents. *Mol. Biol. Evol.* **14:** 823–828.

Roe, B. P. (1992). "Probability and Statistics in Experimental Physics," p. 97, Springer-Verlag, New York.

Sabeur, G., Macaya, G., Kadi, F., and Bernardi, G. (1993). The isochore patterns of mammalian genomes and their phylogenetic implications. *J. Mol. Evol.* **37:** 93–108.

Salinas, J., Zerial, M., Filipski, J., and Bernardi, G. (1986). Gene distribution and nucleotide sequence organization in the mouse genome. *Eur. J. Biochem.* **160:** 469–478.

Schildkraut, C. L., Marmur, J., and Doty, P. (1962). Determination of the base composition of deoxyribonucleic acid from its buoyant density in CsCl. *J. Mol. Biol.* **4:** 430–443.

Simpson, G. G. (1945). The principles of classification and a classification of mammals. *Bull. Am. Mus. Nat. Hist.* **85:** 1–350.

Thiery, J.-P., Macaya, G., and Bernardi, G. (1976). An analysis of eukaryotic genomes by density gradient centrifugation. *J. Mol. Biol.* **108:** 219–235.

Vianey-Liaud, M. (1985). Possible evolutionary relationships among Eocene and lower Oligocene rodents of Asia, Europe and North America. *In* "Evolutionary Relationships among Rodents" (W. P. Luckett and J.-L. Hartenberger, Eds.), pp. 277–309. Plenum, New York.

Viegas-Pequignot, E., Petit, D., Benazzou, T., Prod'homme, M., Lombard, M., Hoffschir, F., Descailleaux, J., and Dutrillaux, B. (1986). Phylogénie chromosomique chez les Sciuridae, Gerbillidae et Muridae, et étude d'espèces appartenant à d'autres familles de Rongeurs. *Mammalia* **50:** 164–202.

Walker, P. M. B. (1968). How different are the DNAs from related animals? *Nature* **219:** 228–232.

Wilson, D. E., and Reeder, D. M. (Eds.) (1993). "Mammal Species of the World: A Taxonomic and Geographic Reference," Random House (Smithsonian Inst. Press), Washington.

Zoubak, S., Clay, O., and Bernardi, G. (1996). The gene distribution of the human genome. *Gene* **174:** 95–102.